Global Journal of Engineering and Technology Advances, 2020, 04(01), 015–029

Global Journal of Engineering and Technology Advances

Cross Ref DOI: 10.30574/gjeta

Journal homepage: http://www.gjeta.com

(RESEARCH ARTICLE)

Fabrication of resistivity meter and its evaluation within shallow depth of investigation

Adegoke Adediran Olanrewaju [1,*], Adiat Kola Abdul Nafiu [2] and Omosuyi Gregory Oluwole [2]

[1] *Department of Physical Sciences (Geophysics programme), Olusegun Agagu University of Science and Technology, Okitipupa, Ondo, Nigeria.*
[2] *Department of Applied Geophysics, Federal University of Technology Akure (FUTA), Ondo, Nigeria.*

Publication history: Received on 19 July 2020; revised on 27 July 2020; accepted on 29 July 2020

Article DOI: https://doi.org/10.30574/gjeta.2020.4.1.0042

Abstract

The high cost of imported and popular resistivity meters has led many geoscientists, geophysical companies and tertiary institutions to go for locally fabricated resistivity meters. These demands and interests in the locally made resistivity meters inspired the authors for solution by designing and fabricating a resistivity meter with voltage and current output. For its evaluation and comparison, the fabricated resistivity meter and ABEM SAS 300 terrameter were used to carry out the same investigations at the same locations in different parts of Nigeria. The investigations carried out involved horizontal profiling (HP), using Wenner configuration and vertical electrical sounding (VES), using Schlumberger configuration. The results obtained are presented as tables, graphs and sounding curves. The RMS errors of the sounding curves generated from VES, range from 2.5 to 4.1. The comparison of the field data obtained from both meters showed good correlation.

Keywords: Resistivity meter; Fabrication; Voltage and current output.

1. Introduction

Procurement of imported resistivity meters by geoscientists, geophysical companies and institutions of higher learning is becoming unaffordable or impossible in Nigeria. This is consequent upon the cost implications, resulting from very high exchange rate, of purchase of the imported resistivity meters, importation duties and logistic of shipment from the manufacturer to the country. This has resulted in many geoscientists, geophysical companies and tertiary institutions developing more interest and demand for locally fabricated resistivity meter. As a result of unavailability of the resistivity meter in many universities in Nigeria, students and researchers usually hire from private companies or agencies [1]. Many times, when these imported meters get damaged, they have to be sent back to the source for repair and this always resulted in waste of financial resources on shipment cost (to and from the manufacturer) and delay in on-going research.

Resistivity meter is used to carry out investigations in electrical resistivity method. Electrical resistivity method has been widely and routinely used for hydrogeological, engineering and environmental investigations [2, 3, 4, 5, 6, 7, 8, 9, 10]. This method utilizes direct currents or low frequency alternating currents. In the resistivity method, artificially-generated electric currents are introduced into the ground through a pair of current electrodes and the resulting potential differences are measured through a pair of potential electrodes at the surface [11] in order to obtain subsurface layers resistivities. Soil resistivity is the key factor that determines what the resistance of a grounding electrode will be [12].

Inspired by the great demand for locally made resistivity meter, the authors have provided solution on how to design, construct and fabricate resistivity meter with voltage and current output for shallow investigation.

* Corresponding author: Adegoke Adediran Olanrewaju

2. Theory of electrical resistivity method

In electrical resistivity survey, electric current (I) is passed into the ground through current electrodes (A and B) and the resulting potential difference (ΔV) is measured between the potential electrodes M and N. The resistivity of the subsurface medium is derived by the division of the values ΔV by I multiplied by the geometric factors of the electrode configuration used.

By considering a cylindrical conductor of length L and a cross sectional area A (Figure 1) with current (I) being passed through it, the resistance (R) can be derived as:

$$R \alpha \frac{L}{A} \quad \text{.....(1)}$$

$$R = \rho \frac{L}{A} \quad \text{.....(2)}$$

where ρ which is the proportionality constant is referred to as the resistivity in ohm-meter (Ω-m). The relationship of the current (I), potential difference (ΔV) and resistance (R) is established by Ohm's law as:

$$\Delta V \alpha I \quad \text{.....(3)}$$

$$\Delta V = IR \quad \text{.....(4)}$$

$$\Delta V / I = R \quad \text{.....(5)}$$

The combination of equation (2) and (5) gives:

$$\rho \frac{L}{A} = \frac{\Delta V}{I}$$

$$\rho = \frac{A \Delta V}{IL} \quad \text{.....(6).}$$

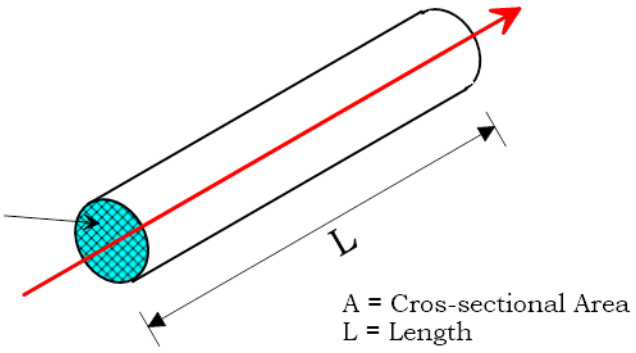

Figure 1 A cylindrical conductor

In electrical resistivity method, four electrodes are mostly used (Figure 2)

The potential at electrode M due to current at electrode A is given as

$$V_{MA} = \frac{I\rho}{2\pi r_1} \quad \text{.....(7)}$$

The potential at electrode M due to current at electrode B is given as

$$V_{MB} = \frac{-I\rho}{2\pi r_2} \quad \text{.....(8)}$$

The potential ($V_{MA,MB}$) at an interval electrode M is the sum of the potential contribution V_{MA} and V_{MB} from the current source A and the sink B respectively:

$$V_{MA,MB} = V_{MA} + V_{MB} \quad \text{.....(9)}$$

$$V_{MA,MB} = \frac{I\rho}{2\pi r_1} + \frac{-I\rho}{2\pi r_2}$$

$$V_{MA,MB} = \frac{I\rho}{2\pi}\left[\frac{1}{r_1} - \frac{1}{r_2}\right] \quad \text{.....(10)}$$

The potential at electrode N due to current at electrode A is given as

$$V_{NA} = \frac{I\rho}{2\pi r_3} \quad \text{.....(11)}$$

The potential at electrode N due to current at electrode B is given as

$$V_{NB} = \frac{-I\rho}{2\pi r_4} \quad \text{.....(12)}$$

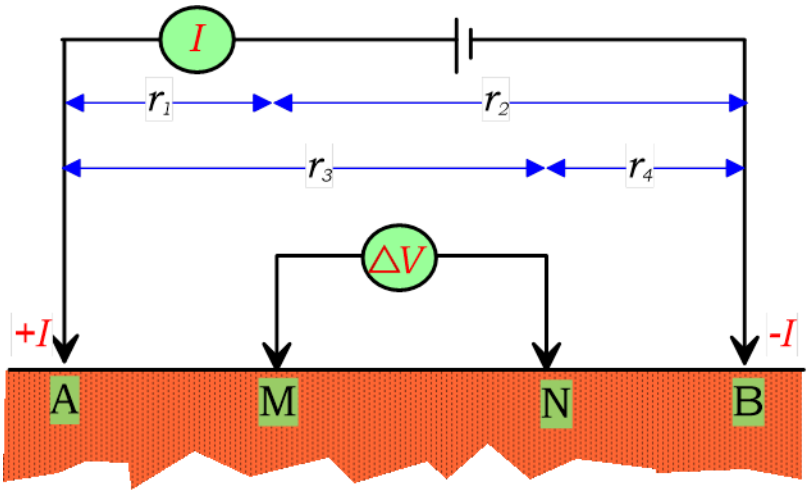

Figure 2 Generalized form of four electrodes configuration.

The potential ($V_{NA,NB}$) at an interval electrode N is also the sum of the potential contribution V_{NA} and V_{NB} from the current source A and the sink B respectively:

$$V_{NA,NB} = V_{NA} + V_{NB} \quad \text{.....(13)}$$

$$V_{NA,NB} = \frac{I\rho}{2\pi r_3} + \frac{-I\rho}{2\pi r_4}$$

$$V_{NA,NB} = \frac{I\rho}{2\pi}\left[\frac{1}{r_3} - \frac{1}{r_4}\right] \quad \text{.....(14)}$$

Since absolute potentials are difficult to monitor, hence the potential difference (ΔV) between electrodes A and B is measured by [11]:

$$\Delta V = V_{MA,MB} - V_{NA,NB} \quad \text{.....(15)}$$

$$\Delta V = \frac{I\rho}{2\pi}\left[\frac{1}{r_1} - \frac{1}{r_2} - \frac{1}{r_3} + \frac{1}{r_4}\right] \quad \text{.....(16)}$$

$$\rho = \frac{2\pi\Delta V}{I}\left[\frac{1}{r_1} - \frac{1}{r_2} - \frac{1}{r_3} + \frac{1}{r_4}\right]^{-1} \quad \text{.....(17)}$$

Since, R = ΔV/I

$$\rho = 2\pi R\left[\frac{1}{r_1} - \frac{1}{r_2} - \frac{1}{r_3} + \frac{1}{r_4}\right]^{-1} \quad \text{.....(18)}$$

This is the generalized resistivity equation for any electrode array system. Equation (18) could also be written as ρ = GR

Where G is the geometric factor of the array.

$$G = \left[\frac{2\pi}{\frac{1}{r_1} - \frac{1}{r_2} - \frac{1}{r_3} - \frac{1}{r_4}}\right] \quad \text{.....(19)}$$

Many electrode arrays (configurations) are employed in resistivity method. Electrode array is the pattern of arrangement of the current and potential electrodes. The most common electrode configurations are Wenner and Schlumberger configurations.

In the Wenner configuration, the inter-electrode spacing (a) is uniform that is AM = MN = NB, which makes $r_1 = r_4 = a$ and $r_2 = r_3 = 2a$ (Figure 3a). Therefore, the equation for apparent resistivity becomes:

$$\rho_a = \frac{2\pi\Delta V}{I}\left[\frac{1}{\frac{1}{a} - \frac{1}{2a} - \frac{1}{2a} + \frac{1}{a}}\right] \quad \text{.....(20)}$$

$$\rho_a = \frac{2\pi a\Delta V}{I} = 2\pi aR \quad \text{.....(21)}$$

In the Schlumberger array, $r_1 = r_4 = L - l$ and $r_2 = r_3 = L + l$(Figure 3b). By substituting for r_1, r_2, r_3 and $r_4$in equation 18, the apparent resistivity gives:

$$\rho_a = \frac{2\pi\Delta V}{I}\left[\frac{1}{\frac{1}{L-l}-\frac{1}{L+l}-\frac{1}{L+l}+\frac{1}{L-l}}\right] \quad \text{.....(22)}$$

$$\rho_a = \frac{2\pi L^2}{2l}.\frac{\Delta V}{I} = \frac{2\pi L^2}{2l}.R \quad \text{.....(23)}$$

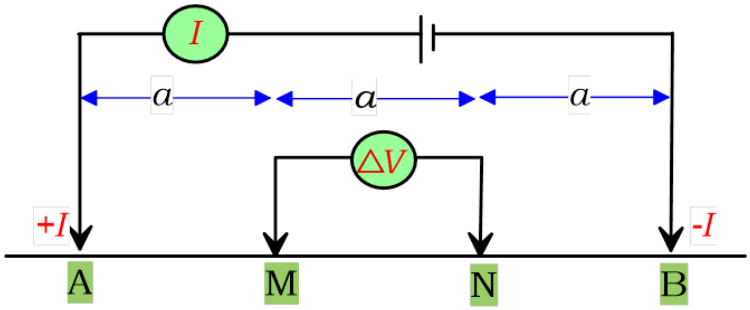

(a) Wenner configuration

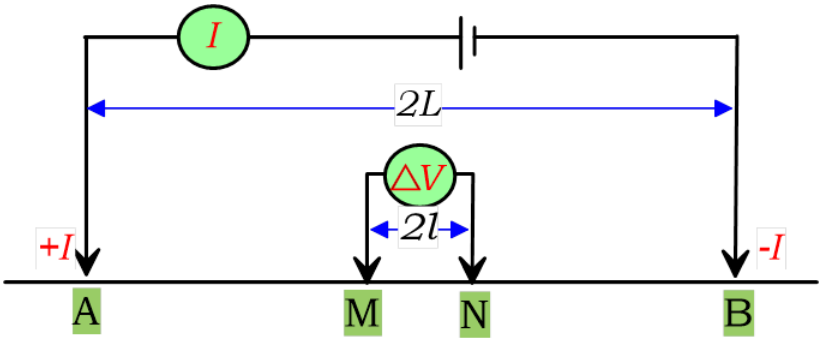

(b) Schlumberger configuration

Figure 3 Wenner and Schlumberger electrodes configuration.

3. Instrumentation

The designed meter is divided into different operation units. These units are power source, inverter, rectification, smoothing and metering. The block and circuit diagrams for the designed meter are shown in Figs. 4 and 5 respectively. A 12V battery was used as the power supply source. The inverter unit was used to convert the low voltage from the direct current (DC) from battery to high voltage alternating current (AC). In the rectification unit, a bridge rectifier was used to produce a full wave rectification. A bridge rectifier can be obtained either by using four separate individual diodes or a specially made one containing four diodes already joined together. Smoothing was carried out by connecting a large value electrolytic capacitor connected across the DC output of rectification unit. This capacitor acts as a reservoir to smoothing the effect of rectification. The metering unit which consists of two multimeter were used in taking the current and the voltage readings separately.

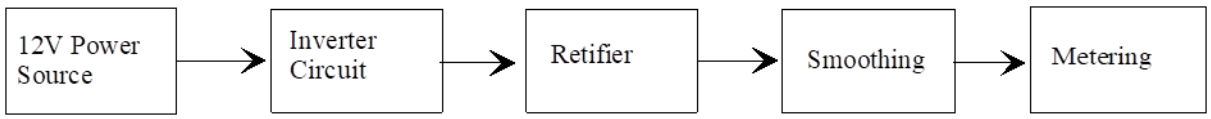

Figure 4 The block diagram for the designed meter.

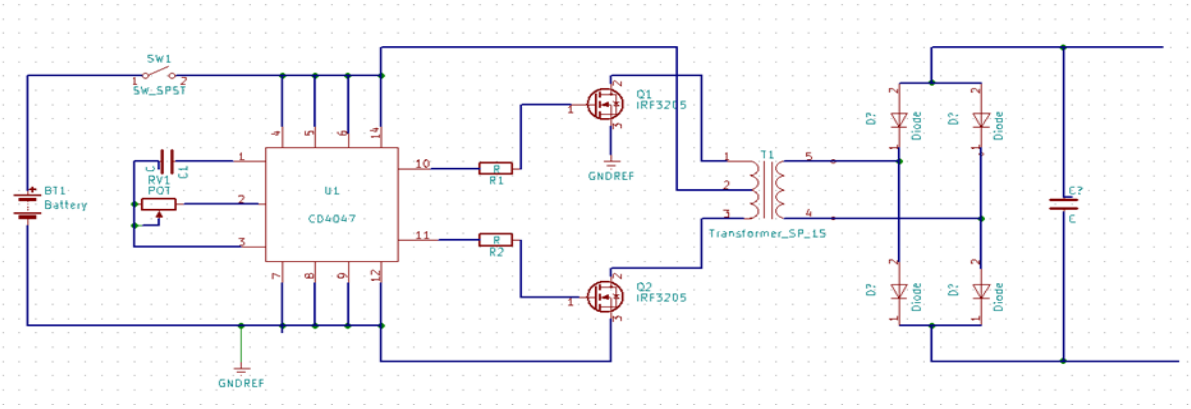

Figure 5 The circuit diagram for the designed meter.

4. Field procedure and techniques

For the field procedure, both the current and potential electrodes were connected to this meter through four reels of wire. The direct current generated from the fabricated resistivity meter was introduced into the ground via currents electrodes by pressing the 'Send' button (Figure 6) on the meter. The resulting potential differences were measured through a pair of potential electrodes. Both the current (I) and voltage (V) readings were read from the two multimeter, set to direct current and direct voltage modes separately. The resistance (R) was then calculated using Ohm's law, which states that V = IR.

Two field techniques were adopted in order to evaluate the fabricated resistivity meter. These were horizontal profiling (HP) and vertical electrical sounding (VES). Horizontal profiling was used to investigate lateral variations in ground resistivity with respect to a particular datum. The VES was used to investigate vertical variations of ground resistivity. Wenner electrode configuration was adopted for HP while Schlumberger configuration was adopted for VES. Inter electrode spacing of a = 10 m was used for the Wenner configuration. A maximum spread of AB/2 = 100 m was used for the Schlumberger configuration.

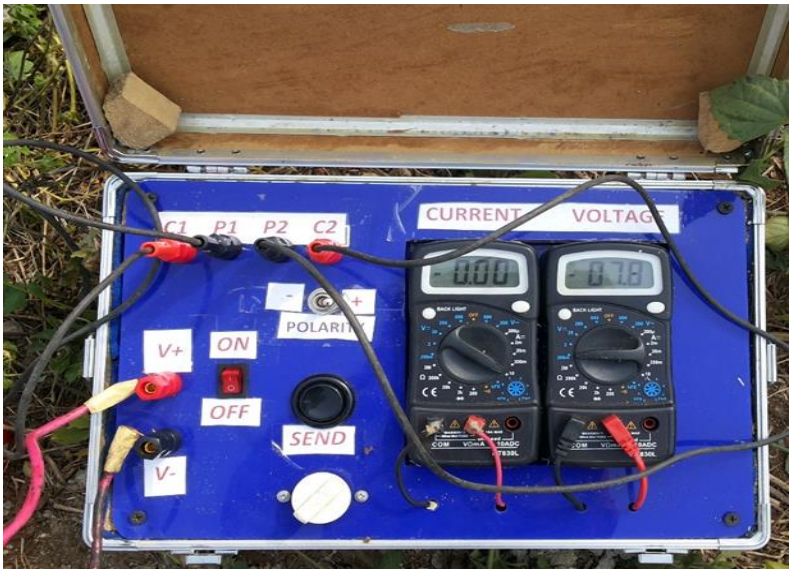

Figure 6 The fabricated resistivity meter**.**

5. Results and discussion

Both the fabricated resistivity meter and the imported ABEM SAS 300 terrameter were used to carry out the same investigations at the same locations in different parts of Nigeria. The different parts of the country investigated span from basement complex to sedimentary rocks environment. The area covered were Ibadan, Ogbomosho, Oyo town, Iseyin, Abeokuta, Ile-Ife, Ado-Ekiti, Akure, Ondo town, Owo, Akungba, Ikare, Ore, Ode-Aye, Okitipupa, Igbotako, Igbokoda, Auchi, Benin, Ikeja and Igarra (Figure 7). A total of fifty-two (52) horizontal profiling and, one hundred and eight (108) vertical electrical soundings were conducted across the study area. The results obtained from the fabricated meter were compared with that of the ABEM SAS 300 terrameter which served as a well-known imported meter. Tables 1 and 2 show the results of the typical field data for the horizontal profiling (HP) from site 3 in Akure. Figures 8 and 9 show the respective graphs of the obtained HP. The typical field data for some of the obtained VES are presented as tables (Tables 3, 4, 5 and 6) and their respective typical sounding curves are shown in Figures10, 11, 12 and 13. The RMS errors of the sounding curves for VES 1A, 1B, 2A and 2B are 3.0, 2.5, 4.2 and 4.1 respectively. The RMS errors of VES 1B and 2B obtained from ABEM terrameter are a little lesser than that of VES 1A and 2A obtained from the fabricated meter.

The relationship between the apparent resistivity data obtained from both meters was established and presented in graph form (Figure 14). The apparent resistivity data for both horizontal profiling and vertical electrical sounding for the fabricated meter were plotted on x-axis against its corresponding apparent resistivity data for the ABEM terrameter on the y-axis. A linear relationship was obtained and a straight line was fitted by regression to obtain coefficient of correlation. About one thousand, eight hundred and ten (1,810) data points were used to generate this graph. The coefficient of correlation (R^2) had a value of 0.993. The high coefficient of correlation established the reliability of the fabricated resistivity meter.

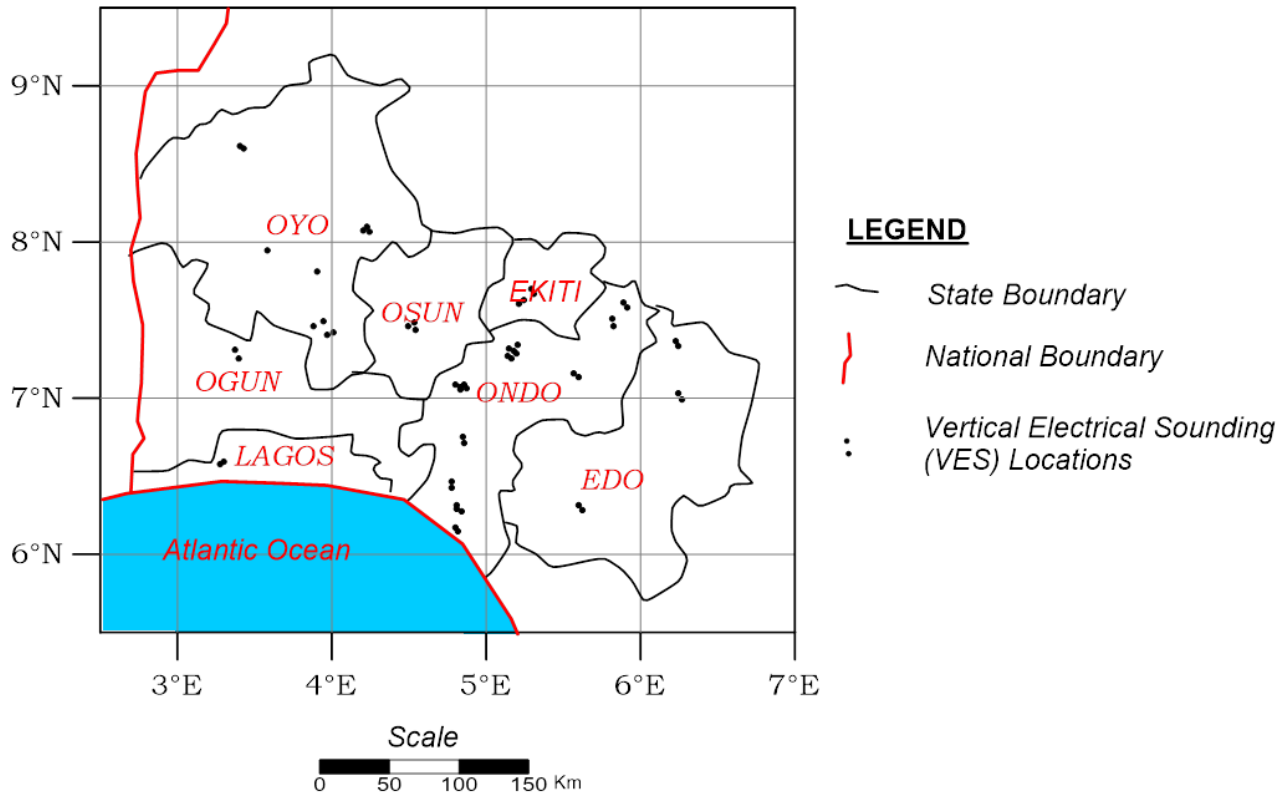

Figure 7 Map of the investigated area.

Table 1 Horizontal profile field data for the fabricated resistivity meter from site 3 (Akure).

Station Midpoint	**Initial Voltage (V_I)**	**Final Voltage (V_F)**	**Current (I)**	**Resistance (R)**	**Apparent Resistivity**
(m)	(mV)	(mV)	(mA)	(ohm)	(Ohm-m)
15	24.1	27.9	12.2	0.31	19.49
25	12.6	16.3	10.8	0.34	21.37
35	51.8	56.7	14.7	0.33	20.74
45	44.4	51.0	14.6	0.45	28.29
55	78.2	82.8	9.6	0.48	30.17
65	11.3	17.5	12.1	0.51	32.06
75	45.9	52.1	15.2	0.41	25.77
85	30.8	36.2	16.3	0.33	20.74
95	33.5	43.1	17.5	0.55	34.57
105	98.2	104.0	11.9	0.49	30.80
115	120.6	127.5	13.0	0.53	33.31

Table 2 Horizontal profile field data for the ABEM terrameter from site 3 (Akure).

Station Midpoint	**Resistance (R)**	**Apparent Resistivity**
(m)	(Ohm)	(Ohm-m)
15	0.35	22.00
25	0.36	22.63
35	0.34	21.37
45	0.48	30.17
55	0.45	28.29
65	0.53	33.31
75	0.44	27.66
85	0.32	20.11
95	0.59	37.09
105	0.51	32.06
115	0.54	33.94

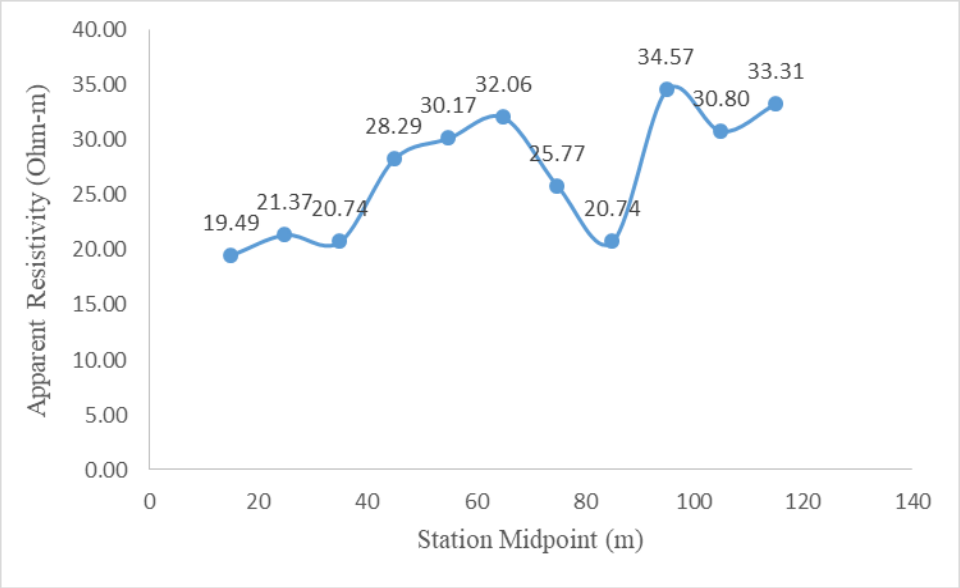

Figure 8 Profile obtained from the fabricated resistivity meter for site 3 (Akure).

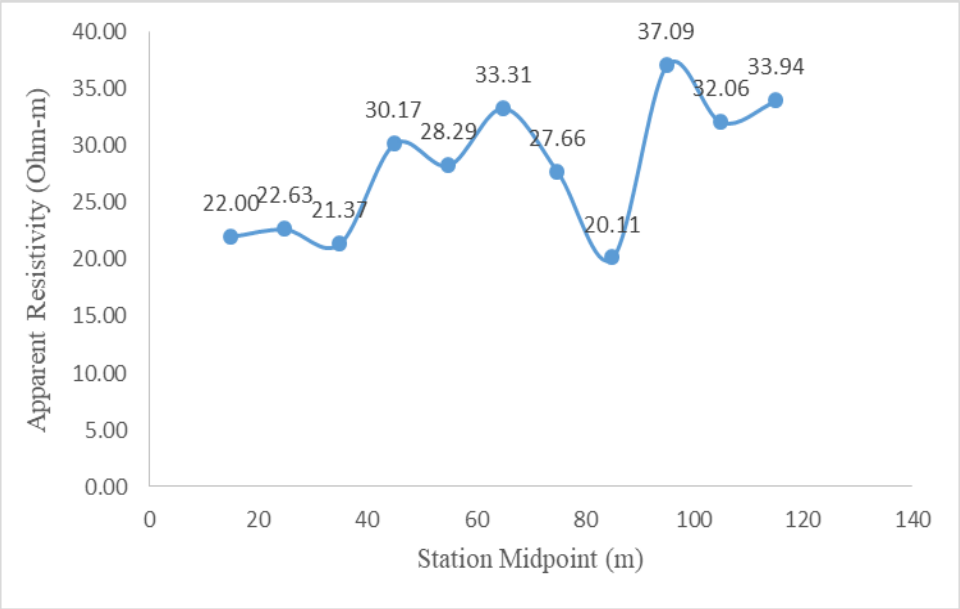

Figure 9 Profile obtained from the ABEM terrameter for site 3 (Akure).

Table 3 VES field data for the fabricated resistivity meter from site 1 (Akure).

Elect. Positn	Half Current Spacing (m)	Half Poten. Spacing (m)	Geom. Factor (G)	Initial Voltage (V_I)	Final Voltage (V_F)	Current (I)	Resistance (ohms)	Apparent Resistivity
	AB/2	MN/2	G	(mV)	(mV)	(mA)	R (ohm)	(Ohm-m)
1	1	0.25	6.28	45.1	366.0	8.8	36.46	229
2	2	0.25	25.13	45.5	259.0	24.5	8.71	219
3	3	0.25	56.55	44.9	88.0	12.3	3.50	198
4	4	0.25	100.53	44.3	73.1	15.1	1.91	192
5	6	0.25	226.19	44.8	58.7	14.1	0.99	223
6	6	0.50	113.10	65.1	95.6	14.1	2.17	245
7	8	0.50	201.06	68.3	86.6	12.8	1.43	287
8	12	0.50	452.39	68.8	75.2	9.4	0.69	310
9	15	0.50	706.86	69.4	74.3	10.5	0.47	330
10	15	1.00	353.43	13.0	22.1	10.6	0.85	302
11	25	1.00	981.75	6.3	9.2	13.1	0.22	220
12	32	1.00	1608.50	4.4	5.7	9.8	0.13	214
13	40	1.00	2513.27	3.5	4.3	11.2	0.07	180
14	40	2.50	1005.31	2.0	4.2	11.2	0.20	198
15	65	2.50	2654.65	15.2	15.8	8.2	0.08	210
16	100	2.50	6283.19	15.6	16.0	7.8	0.05	344

Table 4 VES field data for the ABEM terrameter from site 1 (Akure).

Elect. Positn	Half Current Spacing (m)	Half Poten. Spacing (m)	Geom. Factor (G)	Resistance (ohms)	Apparent Resistivity
	AB/2	MN/2	G	R (ohm)	(Ohm-m)
1	1	0.25	6.28	39.97	251
2	2	0.25	25.13	8.83	222
3	3	0.25	56.55	3.55	201
4	4	0.25	100.53	1.99	200
5	6	0.25	226.19	1.01	228
6	6	0.50	113.10	2.16	244
7	8	0.50	201.06	1.45	291
8	12	0.50	452.39	0.69	312
9	15	0.50	706.86	0.46	322
10	15	1.00	353.43	0.85	300
11	25	1.00	981.75	0.23	225
12	32	1.00	1608.50	0.13	212
13	40	1.00	2513.27	0.07	181
14	40	2.50	1005.31	0.19	190
15	65	2.50	2654.65	0.08	217
16	100	2.50	6283.19	0.06	354

Table 5 VES field data for the fabricated resistivity meter from site 2 (Owo).

Elect. Positn	Half Current Spacing (m)	Half Poten. Spacing (m)	Geom. Factor (G)	Initial Voltage (V_I)	Final Voltage (V_F)	Current (I)	Resistance (ohms)	Apparent Resistivity
	AB/2	MN/2	G	(mV)	(mV)	(mA)	R (ohm)	(Ohm-m)
1	1	0.25	6.28	7.9	1192.0	8.8	134.55	845
2	2	0.25	25.13	7.7	463.0	24.5	18.58	467
3	3	0.25	56.55	7.7	99.9	12.3	7.50	424
4	4	0.25	100.53	7.6	58.8	15.1	3.39	341
5	6	0.25	226.19	7.6	26.6	14.1	1.34	304
6	6	0.50	113.10	34.0	73.1	14.1	2.78	314
7	8	0.50	201.06	33.7	54.1	12.8	1.59	320
8	12	0.50	452.39	33.6	40.3	9.4	0.72	324
9	15	0.50	706.86	33.4	37.7	10.5	0.41	288
10	15	1.00	353.43	97.0	104.9	10.6	0.74	262
11	25	1.00	981.75	96.8	100.0	13.1	0.25	242
12	32	1.00	1608.50	96.8	98.4	9.8	0.16	258
13	40	1.00	2513.27	96.7	97.9	11.2	0.11	269
14	40	2.50	1005.31	12.8	15.8	11.2	0.27	271
15	65	2.50	2654.65	12.8	13.8	8.2	0.12	331
16	100	2.50	6283.19	12.7	13.3	7.8	0.07	444

Table 6 VES field data for the ABEM terrameter from site 2 (Owo).

Elect. Positn	Half Current Spacing (m)	Half Poten. Spacing (m)	Geom. Factor (G)	Resistance (ohms)	Apparent Resistivity
	AB/2	MN/2	G	R (ohm)	(Ohm-m)
1	1	0.25	6.28	130.73	821
2	2	0.25	25.13	18.30	460
3	3	0.25	56.55	7.16	405
4	4	0.25	100.53	3.08	310
5	6	0.25	226.19	1.32	299
6	6	0.50	113.10	2.83	320
7	8	0.50	201.06	1.60	322
8	12	0.50	452.39	0.67	303
9	15	0.50	706.86	0.39	275
10	15	1.00	353.43	0.77	271
11	25	1.00	981.75	0.24	235
12	32	1.00	1608.50	0.16	250
13	40	1.00	2513.27	0.11	273
14	40	2.50	1005.31	0.28	280
15	65	2.50	2654.65	0.14	359
16	100	2.50	6283.19	0.07	461

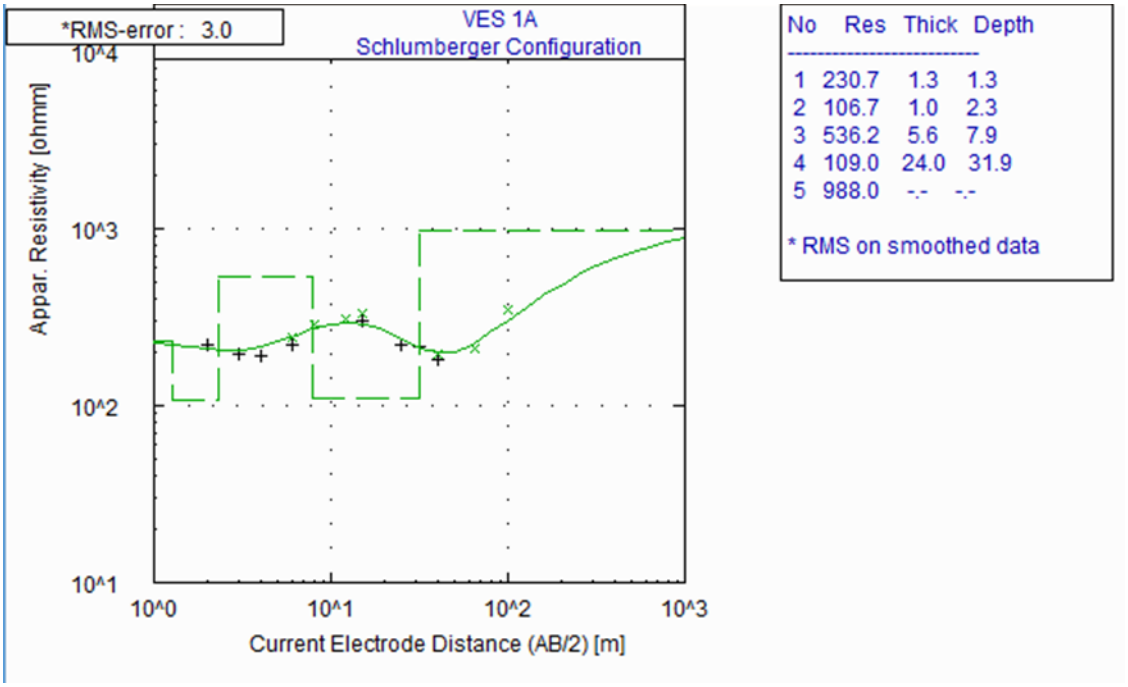

Figure 10 Sounding curve for the fabricated resistivity meter from site 1 (Akure).

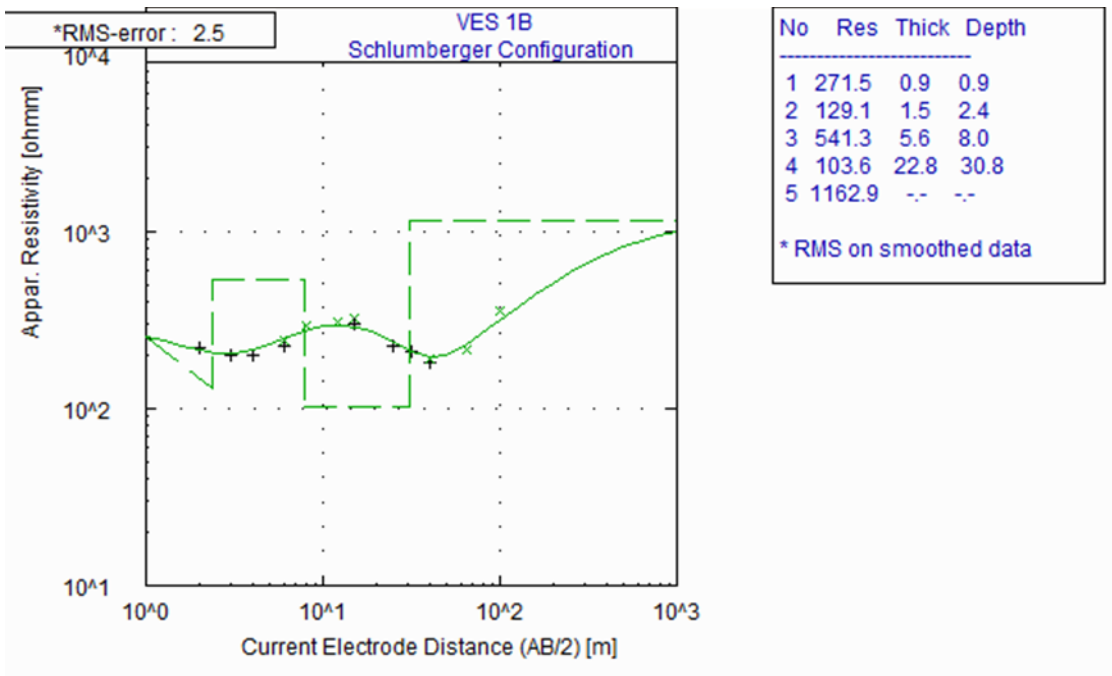

Figure 11 Sounding curve for the ABEM terrameter from site 1 (Akure).

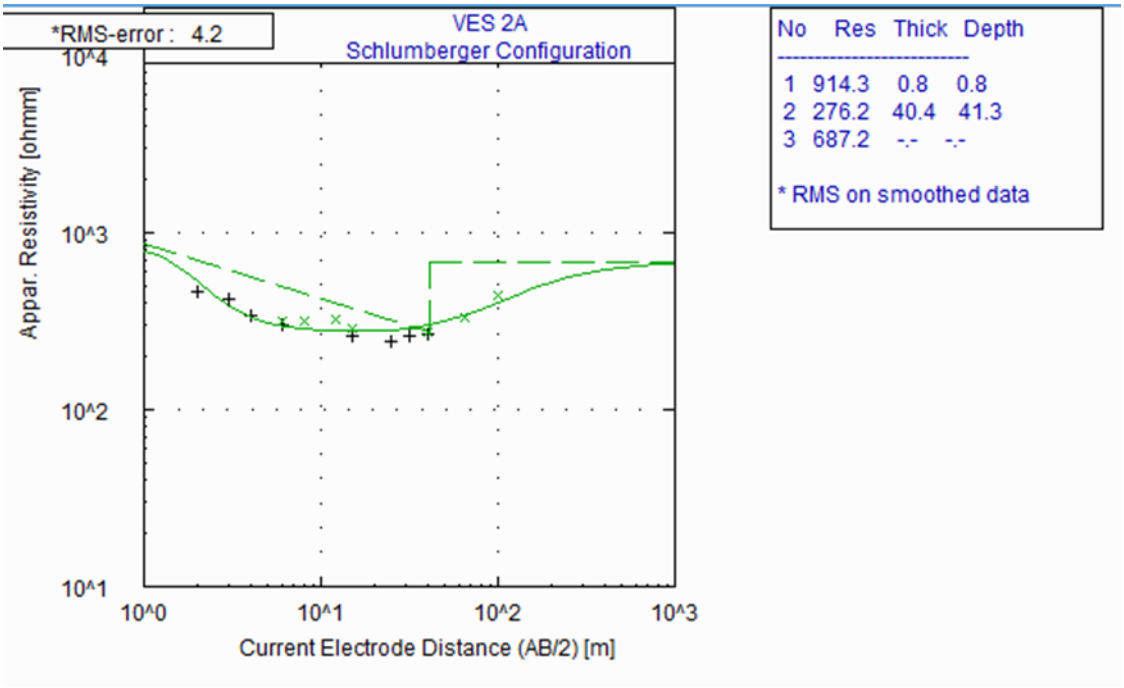

Figure 12 Sounding curve for the fabricated resistivity meter from site 2 (Owo).

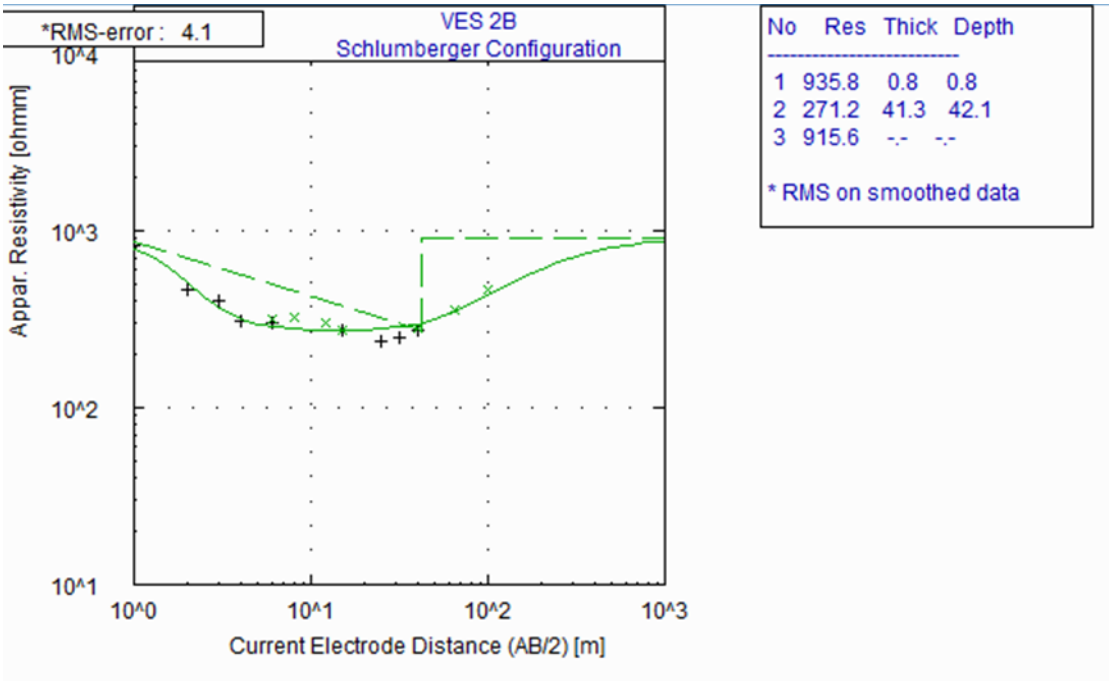

Figure 13 Sounding curve for the ABEM terrameter from site 2 (Owo).

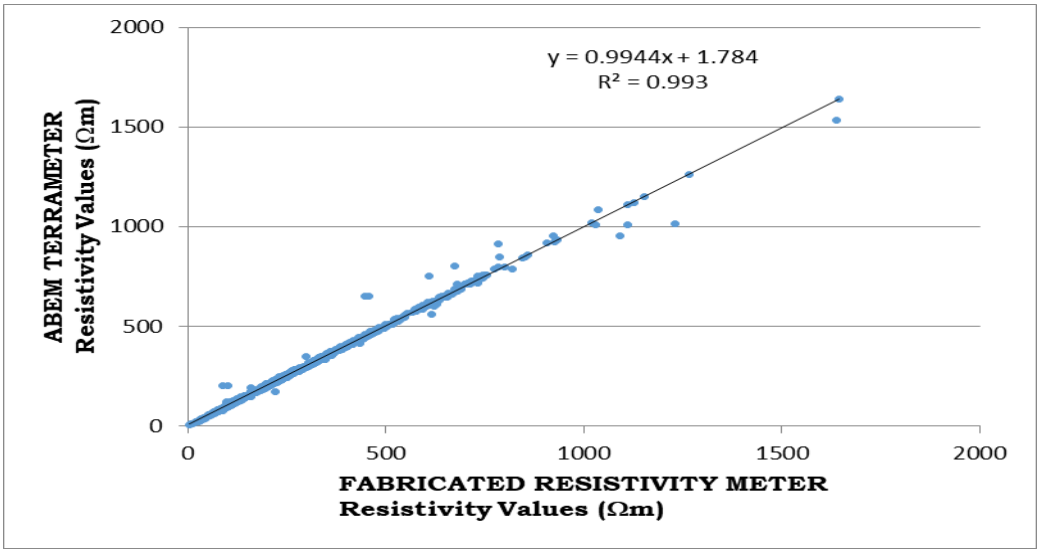

Figure 14 Graph showing relationship between the resistivity data obtained from fabricated resistivity meter and ABEM terrameter.

6. Conclusion

In conclusion, comparison of the results obtained from the fabricated resistivity meter with the imported ABEM SAS 300 terrameter showed good correlation. This has erased the negative thinking that locally made resistivity meters are not accurate and reliable. It should be noted that depth of investigation for this locally made meter here is only for shallow depth investigation (a depth of less than 40m). More researches are going on for fabrication of improved and advanced locally made meter for deeper depth investigation.

Compliance with ethical standards

Acknowledgments

The authors would like to thank every individual that assisted in the data acquisition for this research work.

Disclosure of conflict of interest

All authors declare that there is no conflict of interest regarding the publication of this paper.

References

[1] Awotoye KS and Selemo AOI. (2006). Design and construction of a resistivity meter for Shallow investigation. Nigeria Journal of Physics, 18(2), 261-269.

[2] Barongo JO and Palacky GJ. (1991). Investigations of electrical properties of weathered layers in the Yala area, Western Kenya, using resistivity soundings. Geophys, 56(O.I), 133-138.

[3] Olayinka AI and Olorunfemi MO. (1992). Determination of geoelectrical characteristic in Okene Area and implication for boreholes setting. J. Min. Geol, 28, 403 - 412.

[4] Olorunfemi MO, Ojo JS and Akintunde OM. (1999). Hydrogeophysical evaluation of the groundwater potential of Akure metropolis, southwestern Nigeria. J. Min. Geol, 35(2), 207-228.

[5] Omosuyi GO, Adegoke AO and Adelusi AO. (2008). Interpretation of Electromagnetic and Geoelectric Sounding Data for Groundwater Resources around Obanla-Obakekere, near Akure, Southwestern Nigeria. The Pacific Journal of Science and Technology, 9(2), 508-525.

[6] Akinlalu AA, Adegbuyiro A, Adiat KAN, Akeredolu BE and Lateef WY. (2017). Application of multi-criteria decision analysis in prediction of groundwater resources potential: A case of Oke-Ana, Ilesa Area Southwestern, Nigeria. NRIAG Journal of Astronomy and Geophysics, 6, 184–200.

[7] Adiat KAN, Ajayi OF, Akinlalu AA and Tijani IB. (2020). Prediction of groundwater level in basement complex terrain using artificial neural network: a case of Ijebu-Jesa, southwestern Nigeria. Applied Water Science, 10, 8.

[8] Olayanju Gbenga M, Adelusi Adebowale O and Adiat Kola AN. (2015). Combined Use of Ground Magnetic and Electrical Resistivity Methods in Bedrock Mapping: Case Study of NTA Premises, Oba Ile Area, South-Western Nigeria. Electronic Journal of Geotechnical Engineering, Vol. 20 [2015], Bund. 15, 6591-6606.

[9] Adiat KAN, Akinlalu AA and Adegoroye AA. (2017). Evaluation of road failure vulnerability section through integrated geophysical and geotechnical studies. NRIAG Journal of Astronomy and Geophysics, 6, 244–255.

[10] Adeyemo IA and Omosuyi GO. (2012). Geophysical Investigation of Road Pavement Instability along part of Akure-Owo express way, Southwestern Nigeria. Am. J. Sci. Ind.Res, 3(4), 191-197.

[11] Kearey P, Brooks M and Hill I. (2002). An introduction to geophysics exploration. 3rd Edn., Blackwell Science, Letchworth, U.K, 183-196.

[12] Igboama WN and Ugwu NU. (2011). Fabrication of resistivity meter and its evaluation. Am. J. Sci. Ind. Res, 2(5), 713-717.

How to cite this article

Adegoke AO, Adiat KAN and Omosuyi GO. (2020). Fabrication of resistivity meter and its evaluation within shallow depth of investigation. Global Journal of Engineering and Technology Advances, 4(1), 15-29.